Polarimetric Direct Detection for Spatial Superchannels

Jaroslaw Kwapisz
Department of Mathematical Sciences
Montana State University
Bozeman, MT
jkwapisz@montana.edu

Ioannis Roudas
Electrical and Computer Engineering
Montana State University
Bozeman, MT
ioannis.roudas@montana.edu

Eric Fink
Department of Mathematical Sciences
Montana State University
Bozeman, MT
eric.fink@montana.edu

***Abstract*—Polarimetric direct-detection receivers can retrieve amplitude and phase information sent jointly over the components of a spatial superchannel. Exploiting the interdependence of Stokes parameters, we propose an optimized receiver design where the photodiode count increases linearly with the number of spatial degrees of freedom.**

***Index Terms*—Optical interconnects, modulation formats, direct detection, short-reach transmission, Stokes vector receiver**

I. Introduction

Short-haul links for 100 Gigabit Ethernet and beyond currently employ M-ary pulse amplitude modulation (M-PAM) and direct detection [1]. The main disadvantage of M-PAM is that its energy consumption scales quadratically with the number of amplitude levels M [2], since the M-PAM constellation is one-dimensional. To accommodate future traffic demands in short-haul optical links, spectral efficiency should be increased. The adoption of modulation formats with signal space dimensionality larger than unity will allow scaling spectral efficiency in a more energy-efficient manner than in the case of M-PAM.

One of the most active research areas in contemporary optical communications is the design of self-homodyne receivers [3]–[5] that can be used in conjunction with energy- and spectrally-efficient higher-dimensional modulation formats. Out of several competing designs proposed over the last few years, Stokes-vector receivers, in particular, have drawn significant attention [3]. In these receivers, self-homodyning is achieved by i) forming various linear superpositions of the x- and y-polarization components of the optical wave after performing polarization rotations; and ii) using multiple photodiodes, acting as square-law detectors, to measure the square moduli of these superpositions. The latter contain beating products that preserve the amplitude and phase information of the received optical wave (apart from a common phase).

As the name 'Stokes-vector' indicates, apart from detecting advanced modulation formats encoded jointly in the x- and y-polarization components, such a receiver has the capability of retrieving the state of polarization of the received optical signal. Therefore, it is possible to use it together with digital polarization modulation formats, such as polarization shift keying (PolSK) [6], [7] and Stokes vector modulation (SVM) [8]–[11]. In addition, this receiver can track and adaptively compensate for random polarization fluctuations induced by birefringence and random coupling in optical fibers.

Funding proved by AFRL Grant FA8750-20-1-1004 PCSN T04257.

Ji et al. [12] recently extended the concept of Stokes-vector detection to optical links employing multimode optical fibers. We refer to this receiver here as a *mode-vector (MV) direct-detection (DD) receiver* to distinguish it from its single-mode-fiber counterpart. The MV receiver can be used, for instance, to detect Mode Vector Modulation (MVM), a generalized polarization modulation scheme proposed by the authors for transmission over multimode/multicore optical fibers or free space [13], [14].

The most rudimentary implementation of the MV receiver for the detection of generalized Stokes vectors requires a set of $2N^2 - N$ identical photodiodes. The drawback of this implementation is that its complexity scales quadratically with N. In this paper, we propose a new MV direct-detection receiver architecture that takes advantage of the interdependence of the generalized Stokes parameters to reduce the front-end complexity to $O(N)$. In the following, we show that $5N - 4$ photodiodes are sufficient to estimate the Stokes parameters of the spatial superchannel.

As an example, we compare the performance of MV receivers with $O(N)$ and $O(N^2)$ hardware complexity, respectively, in the case of optimized MVM constellations [13], [14] of various cardinalities. We show that the reduction in receiver complexity results in no decrease in MVM performance in the amplified-spontaneous-emission (ASE)-noise-limited regime.

II. Preliminaries & Transmitter Architecture

MVM generalizes SVM to multimode and multicore fibers as well as free-space transmission. This M-ary modulation format consists of sending pulses of differing amplitudes and initial phases (but the same shape) over N spatial degrees of freedom, e.g., the x- and y-polarization states within each mode or core.

Each of the signals at the fiber input is described as $\mathbf{E}_m(t) = A_m \exp(i\phi_m) g(t) \left|s_m\right\rangle$ for $m = 1, \ldots, M$, where A_m and ϕ_m are the common amplitude and phase, $g(t)$ is a real-valued function describing the pulse shape, and $\left|s_m\right\rangle$

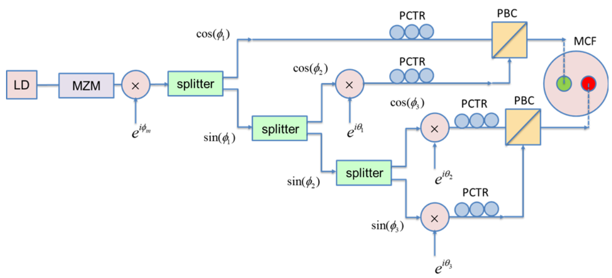

Figure 1. Example MV transmitter architecture for $N = 4$ with a two-core fiber. Symbols: LD=laser diode, MZM=Mach-Zehnder modulator, X=phase modulator, PCTR=polarization controller, PBC=polarization beam combiner.

is a generalized unit Jones vector describing the complex excitations over the N degrees of freedom. Without loss of generality, we assume in this paper that A_m and ϕ_m are constant, focusing on the version of MVM that generalizes PolSK to higher dimensions.

In order to generate the N spatial and polarization components of an MVM signal, the transmitter architecture (e.g., Fig. 1 for $N = 4$) begins with a single semiconductor laser followed by a Mach-Zehnder modulator and a phase modulator to alter the pulse shape $g(t)$, the common amplitude A_m, and common phase ϕ_m. Electro-optic splitters partition the signal into N parallel branches, with the control voltage of each Y-junction being adjusted to create an arbitrary power splitting ratio between its outputs as per the magnitude of the components of $|s_m\rangle$. Phase modulators are then used on each branch to generate the phase differences of $|s_m\rangle$, before using polarization controllers and beam combiners to merge pairs of signals from different optical paths into orthogonal polarization states that are launched into separate fiber cores. This design requires only N phase modulators and polarization controllers, $N-1$ electro-optical splitters, $N/2$ polarization beam combiners, and a single semiconductor laser and Mach-Zehnder modulator.

III. Proposed Receiver Architecture

In this section, we shall use the generalized Jones/Stokes formalism [15] to optimize the architecture of the MV receiver.

The generalized Jones and Stokes vectors $|s\rangle$, $\hat{s}$ can be expressed in terms of their components as $|s\rangle = \begin{bmatrix} s_1 & s_2 & \dots & s_N \end{bmatrix}^T$, and $\hat{s} = \begin{bmatrix} S_1 & S_2 & \dots & S_{N^2-1} \end{bmatrix}^T$, respectively, where T denotes the matrix transpose. The Stokes components are given by the quadratic form [15]

$$S_k = C_N \langle s|\mathbf{\Lambda}_k|s\rangle , \tag{1}$$

where C_N denotes the normalization coefficient [15] $C_N := \sqrt{N/\left[2\left(N-1\right)\right]}$ and $\mathbf{\Lambda}_k$ are the generalized Gell-Mann matrices [16].

By substituting the explicit form of $\mathbf{\Lambda}_k$ into (1), we find that Stokes components can take three distinct forms, as shown in Table I. The purpose of the optical front-end of the receiver is to measure the constituent terms of the equations listed in Table I. Subsequently, this information is provided to the digital signal processing (DSP) unit that computes the Stokes components.

TABLE I. Stokes parameters in terms of the Jones vector components

Number of terms	Indices	Expression
$\frac{N(N-1)}{2}$	$1 \le k \le \frac{N(N-1)}{2}$, $1 \le i < j \le N$	$S_k = 2C_N \Re\{s_i s_j^*\}$
$\frac{N(N-1)}{2}$	$\frac{N(N-1)}{2} + 1 \le k \le N(N-1)$, $1 \le i < j \le N$	$S_k = -2C_N \Im\{s_i s_j^*\}$
$N-1$	$N(N-1)+1 \le k \le N^2-1$, $1 \le \ell \le N-1$	$S_k = C_N \sqrt{\frac{2}{\ell(\ell+1)}} \cdot \left(\sum_{j=1}^{\ell} \lvert s_j\rvert^2 - \ell \lvert s_{\ell+1}\rvert^2 \right)$

Let us examine the calculation of the first two Stokes parameter types in Table I. For each pair of Jones components s_i, s_j, we need to compute the real and imaginary parts of the quantity $s_i s_j^*$. This task can be accomplished by using a 90° optical hybrid followed by two balanced receivers [17], as shown in Fig. 2. We can use $N(N-1)/2$ such units to compute the real and imaginary parts of $s_i s_j^*$, $\Re\{s_i s_j^*\}$, $\Im\{s_i s_j^*\}$, respectively, for all distinct combinations of s_i, s_j (with no regard to order). Since four photodiodes accompany each 90° optical hybrid, presumably a total of $2N^2 - 2N$ photodiodes are required.

Moreover, to compute the third type of Stokes component listed in Table I, we must measure the square moduli of the Jones components $|s_i|^2$ using N photodiodes.

Based on the above, we are compelled to conclude that a grand total of $2N^2 - N$ photodiodes is necessary for the measurement of the (N^2-1) components of the Stokes vector.

This reasoning is flawed, however, because it ignores the fact that the $N^2 - 1$ Stokes are functions of the N Jones components and, therefore, are interdependent. We can take advantage of the interdependence of the generalized Stokes components to reduce the photodiode count of the MV receiver to $O(N)$.

Indeed, we note that measuring the real and imaginary parts of all $N(N-1)/2$ products $s_i s_j^*$ is unnecessary. Two different products $s_i s_j^*$, $s_j s_k^*$ contain common information since they share a common Jones component s_j. This underlying philosophy guides us to adopt the simplified receiver architecture shown in Fig. 3a, composed of a cascade of unit cells like the

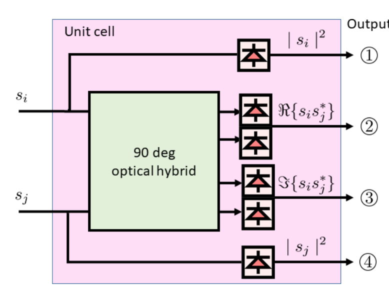

Figure 2. Unit cell architecture. Polarization controllers are placed before the optical hybrid when necessary to align the states of polarization of the $i-$th and $j-$th Jones components.

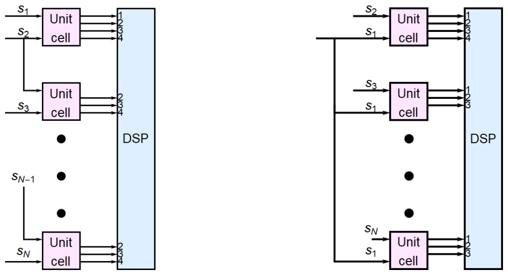

(a) (b)

Figure 3. Schematics of the proposed optically-preamplified MV DD receiver: (a) Cascaded architecture; (b) Self-homodyne architecture.

one shown in Fig. 2. Each unit cell has two inputs s_i, s_j and can measure the characteristic quantities $|s_i|^2$, $|s_j|^2$, $\Re\{s_i s_j^*\}$, and $\Im\{s_i s_j^*\}$. The trick in the simplified receiver architecture of Fig. 3a is that we measure the characteristic quantities of only $(N-1)$ pairs, namely $\{(s_i, s_{i+1}) \mid i = 1, \ldots, N-1\}$. The DSP can then compute the quantities $|s_i|$, $|s_{i+1}|$, and $s_i s_{i+1}^* = \Re\{s_i s_{i+1}^*\} + i\Im\{s_i s_{i+1}^*\}$. From the latter, we have at our disposal the differential phases $\theta_{i,i+1} := \theta_i - \theta_{i+1} = \arg\left(s_i s_{i+1}^*\right)$. Thus, we can recover all terms $s_i s_j^*$ by

$$s_i s_j^* = e^{i\theta_{i,j}} |s_i||s_j|, \tag{2}$$

where, for any $i < j$, $\theta_{i,j} := \theta_{i,i+1} + \cdots + \theta_{j-1,j}$.

A variant of the simplified receiver architecture depicted in Fig. 3a is shown in Fig. 3b. Again we measure the characteristic quantities of only $(N-1)$ pairs, but this time we use s_1 as a common reference, i.e., $s_i s_1^*$, $i = 2, \ldots, N$. If we do not send data over the first spatial and polarization degree of freedom, s_1 is a (non-zero) constant and can be used to recover the moduli and relative phases of all other Jones components. We realize that this is a true self-homodyne receiver, essentially equivalent to a coherent homodyne phase diversity receiver, except that we replaced the local oscillator input with a reference wave sent by the transmitter. Sacrificing one of the degrees of freedom at our disposal allows the use of multidimensional modulation formats previously proposed only for coherent detection [18], [19].

The hardware implementation of the MV receivers of Fig. 3a, 3b requires cascading $(N-1)$ unit cells like the one shown in Fig. 2. The first unit cell uses six photodiodes but for the remaining $N-2$ unit cells, only five photodiodes are required. A grand total of $5N-4$ photodiodes is necessary for the measurement of the (N^2-1) components of the Stokes vector. Thus, the front-end complexity increases linearly with the number N of the spatial and polarization degrees of freedom. Furthermore, it is possible to resort to single-ended detection for the outputs 2 and 3 of the unit cell to reduce hardware complexity to the absolute minimum. Then, only $3N-2$ photodiodes are required to estimate the Stokes parameters.

IV. Results and Discussion

One might hypothesize that the linearized-hardware-complexity MV receivers presented in the previous section will unavoidably suffer from the accumulation of numerical errors in the estimation of S_i, since one must combine several noisy measurements to calculate all terms $s_i s_j^*$. In this section, we use Monte Carlo simulation to check this hypothesis. More specifically, we compare the performance of the receiver architecture shown in Fig. 3a against the one of the 'naïve' mode-vector receiver based on $2N^2-N$ photodiodes. For this comparison, we consider the detection of simplex MVM constellations based on symmetric, informationally complete, positive operator-valued measure (SIC-POVM) vectors, as well as other geometrically-optimized constellations [13], [14].

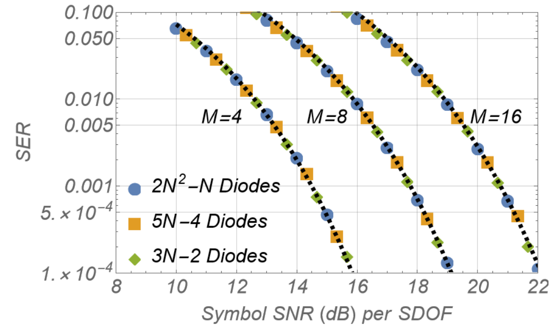

(a) $N = 2$

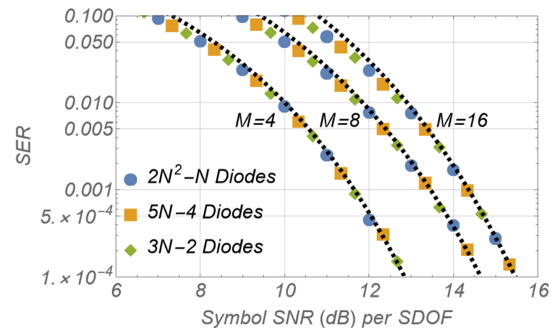

(b) $N = 4$

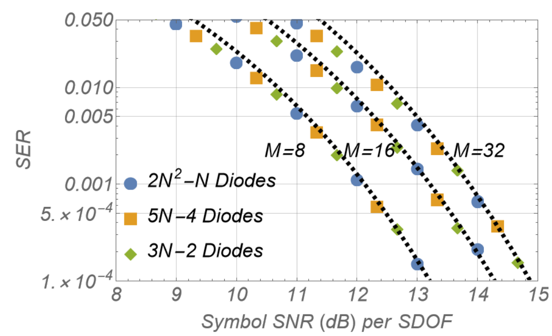

(c) $N = 8$

Figure 4. Performance comparison of MV receivers with $O(N)$ and $O(N^2)$ hardware complexity using Monte Carlo simulation: SER vs symbol SNR per spatial degree of freedom (SDOF) in the exclusive presence of ASE noise for various (N, M)-MVM constellations.

Fig. 4 shows the symbol error rate (SER) vs symbol signal-to-noise ratio (SNR) per spatial degree of freedom (SDOF) of the various receiver architectures, in the exclusive presence of ASE noise, computed using Monte Carlo simulation. We obtain identical performance for the quadratic- and linear-complexity receivers. The study of the performance in the presence of device imperfections and electrical noise is left for future work.

V. Summary

We proposed a new MV direct-detection receiver architecture that takes advantage of the interdependence of Stokes parameters so that its complexity increases linearly with the number of spatial degrees of freedom. As an example, we showed that the reduction in hardware complexity results in no penalty in performance when the receiver is used in conjunction with (N, M)-MVM constellations in the ASE-noise-limited regime.

References

[1] X. Pang, O. Ozolins, R. Lin, L. Zhang, A. Udalcovs, L. Xue, R. Schatz, U. Westergren, S. Xiao, W. Hu, G. Jacobsen, S. Popov, and J. Chen, "200 Gbps/lane IM/DD technologies for short reach optical interconnects," *J. Lightw. Technol.*, vol. 38, pp. 492–503, Jan. 2020.

[2] J. Proakis, *Digital Communications 5th Edition*. Boston: McGraw-Hill, 2007.

[3] X. Chen, C. Antonelli, A. Mecozzi, D. Che, and W. Shieh, "High-capacity direct-detection systems," in *Optical Fiber Telecommunications VII*, pp. 419–441, Elsevier, 2020.

[4] Y. Yoshida, T. Umezawa, A. Kanno, and N. Yamamoto, "A Phase-Retrieving Coherent Receiver Based on Two-Dimensional Photodetector Array," *J. Lightw. Technol.*, vol. 38, pp. 90–100, Jan. 2020.

[5] H. Chen, N. K. Fontaine, J. M. Gene, R. Ryf, D. T. Neilson, and G. Raybon, "Dual Polarization Full-Field Signal Waveform Reconstruction Using Intensity Only Measurements for Coherent Communications," *J. Lightw. Technol.*, vol. 38, pp. 2587–2597, May 2020.

[6] S. Betti, F. Curti, G. De Marchis, and E. Iannone, "Multilevel coherent optical system based on Stokes parameters modulation," *J. Lightw. Technol.*, vol. 8, no. 7, pp. 1127–1136, 1990.

[7] S. Benedetto and P. Poggiolini, "Theory of polarization shift keying modulation," *IEEE Trans. Commun.*, vol. 40, pp. 708–721, Apr. 1992.

[8] K. Kikuchi and S. Kawakami, "Multi-level signaling in the Stokes space and its application to large-capacity optical communications," *Opt. Express*, vol. 22, p. 7374, Mar. 2014.

[9] D. Che, A. Li, X. Chen, Q. Hu, Y. Wang, and W. Shieh, "Stokes vector direct detection for linear complex optical channels," *J. Lightw. Technol.*, vol. 33, pp. 678–684, Jan. 2015.

[10] M. Morsy-Osman, M. Chagnon, and D. V. Plant, "Four-dimensional modulation and Stokes direct detection of polarization division multiplexed intensities, inter polarization phase and inter polarization differential phase," *J. Lightw. Technol.*, vol. 34, pp. 1585–1592, Apr. 2016.

[11] T. Tanemura and Y. Nakano, "Compact InP Stokes-vector modulator and receiver circuits for short-reach direct-detection optical links," *IEICE Transactions on Electronics*, vol. E101.C, pp. 594–601, July 2018.

[12] H. Ji, D. Che, C. Sun, J. Fang, G. Milione, R. R. Unnithan, and W. Shieh, "High-dimensional Stokes vector direct detection over few-mode fibers," *Optics Letters*, vol. 44, p. 2065, Apr. 2019.

[13] I. Roudas, J. Kwapisz, and E. Fink, "Mode vector modulation," in *European Conference on Optical Communication (ECOC)*, Sept. 2021. Paper TuE3.2.

[14] E. Fink, J. Kwapisz, and I. Roudas, "Optimized SVM constellations for SDM fibers," in *IEEE Photonics Conference*, Oct. 2021. Paper TuE3.2.

[15] I. Roudas and J. Kwapisz, "Stokes space representation of modal dispersion," *IEEE Photon. J.*, vol. 9, no. 5, pp. 1–15, 2017.

[16] Wikipedia contributors, "Gell-mann matrices," 2022.

[17] T. Tanemura, T. Suganuma, and Y. Nakano, "Sensitivity analysis of photonic integrated direct-detection Stokes-vector receiver," *J. Lightw. Technol.*, vol. 38, pp. 447–456, Jan. 2020.

[18] T. A. Eriksson, P. Johannisson, B. J. Puttnam, E. Agrell, P. A. Andrekson, and M. Karlsson, "K-over-L multidimensional position modulation," *J. Lightw. Technol.*, vol. 32, no. 12, pp. 2254–2262, 2014.

[19] B. J. Puttnam, T. A. Eriksson, J.-M. D. Mendinueta, R. S. Luís, Y. Awaji, N. Wada, M. Karlsson, and E. Agrell, "Modulation formats for multi-core fiber transmission," *Opt. Express*, vol. 22, p. 32457, Dec. 2014.